Available online at www.sciencedirect.com
ScienceDirect
Carbohydrate Research 342 (2007) 243–253
Carbohydrate RESEARCH

Crystal structure and NMR spectroscopy of aldonamides derived from D-*glycero*-D-*gulo*-heptono-1,4-lactone

Alejandro J. Metta-Magaña,* Reyna Reyes-Martínez and Hugo Tlahuext

Centro de Investigaciones Químicas, Universidad Autónoma del Estado de Morelos, Av. Universidad 1001, Cuernavaca, Morelos, México, CP 62209, Mexico

Received 4 May 2006; received in revised form 13 November 2006; accepted 14 November 2006
Available online 22 November 2006

Abstract—We report the preparation of 12 aldonamides derived from D-*glycero*-D-*gulo*-heptono-1,4-lactone, their NMR characterization and study (^{13}C, ^{1}H, ^{15}N NMR) in Me_2SO-d_6 solution. The evaluation of the coupling constants $^{3}J_{H,H}$ has shown that the sugar chain conformation in solution is all-trans for the studied amides. Because some amides crystallized, we discussed the crystal packing and found motifs. The conformation of the amides in the crystal structures displays two sickles at C2 and C3, with the exception of one that is all-trans. The bends cause the formation of the mean planes C1–C2–C3 and C3–C4–C5–C6–C7 with an average interplanar angle of 88°. We found three main kinds of crystal packing depending on the N-substituent; head-to-tail, bilayer and pseudo-hexagonal mode, all the three show hydrogen-bonding networks that stabilize the crystal lattice.

Keywords: Aldonamides; Conformation; ^{15}N NMR; Crystal packing; Hydrogen bonding

1. Introduction

Aldonamides are usually obtained by reaction of amines with aldonic acids or the related aldonolactones.[1] These compounds have several applications, such as sugar substitutes,[2] extreme pressure additives,[3] raw materials in polymer preparation,[4] and as gelators.[5] Due to these applications, the determination of their conformation in solution and solid state is of interest.

Conformational studies in solution of polyols via NMR spectroscopy have shown that when an unfavorable 1,3-syndiaxial interaction is present, the conformation must be bent[6] unless a hydrogen bond could be formed between these hydroxyl groups, especially when there is more than one bending.[7] On the other hand, the study of crystalline structures are scarce, as is shown by the number of aldonamides' structures in the CCDC database;[8] prevailing N-substituents with longer than six carbon atoms chains, because of their amphiphilic character.

Therefore, it is important to get more data about the effect in the packing owing to different substituents at the amide nitrogen atom. This led us to synthesize the aldonamides **1**–**12** derived from D-*glycero*-D-*gulo*-heptono-1,4-lactone with different N-substituents (Chart 1).

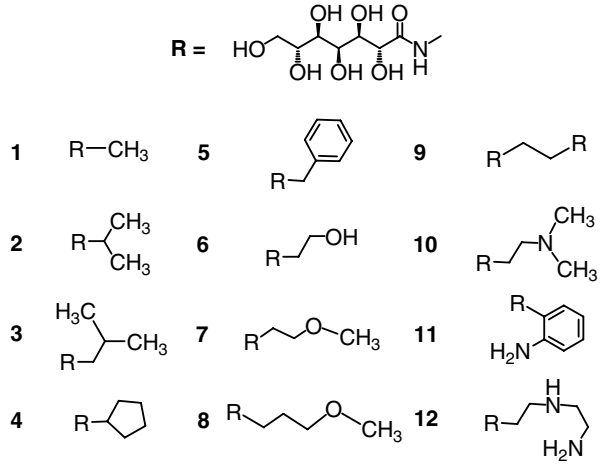

Chart 1. Family of the D-glucoheptonamides (**1**–**12**) synthesized.

* Corresponding author. Tel./fax: +52 777 3 29 79 97; e-mail: memaljo@yahoo.com

0008-6215/$ - see front matter © 2006 Elsevier Ltd. All rights reserved.
doi:10.1016/j.carres.2006.11.020

We were interested in the assignment and study of the NMR data of these amides, because our objective was to determine the preferred conformation in solution for them. We were also concerned about the nature and size of the N-substituent and its effect on the packing of these amides in the solid state, this guided us to study the hydrogen bonds and patterns generated by them.

2. Results and discussion

2.1. NMR analysis in solution

Compounds **1**–**12** (Chart 1) were synthesized by reaction of the corresponding amine with D-*glycero*-D-*gulo*-heptono-1,4-lactone and their structures were confirmed by ^{1}H and ^{13}C NMR spectroscopy. In order to make an unambiguous assignment, we used 2-D NMR experiments such as HOM-2DJ, HETCOR, COSY, HSQC, and ^{15}N HSQC.

The coupling constants $^{3}J_{H,H}$ (Table 1) were obtained through HOM-2DJ experiment and they showed similar values for all the compounds. It points out that the average conformation adopted by the skeleton of the glucohepton moiety does not show a significant change with regard to the N-substituents, and that there exists a preference for a specific conformation.

The mean values for $^{3}J_{2,3}$ (6.3 Hz) and $^{3}J_{5,6}$ (7.6 Hz) correspond to an anti orientation, while the mean values for $^{3}J_{3,4}$ (2.4 Hz) and $^{3}J_{4,5}$ (2.1 Hz) refer to a syn orientation. These hydrogen orientations, together with quiral configuration (2*R*,3*R*,4*S*,5*R*,6*R*), allowed us to

Table 1. NMR data for the glucohepton moiety of the D-glucoheptonamides **1**–**12**

	1	2	3	4	5	6	7	8	9	10	11	12
^{13}C Chemical shifts[a]												
C1	174.3	172.8	173.8	173.2	173.7	173.8	173.3	173.7	174.2	173.6	172.5	173.9
C2	72.7	72.6	72.4	72.5	72.6	72.5	72.4	72.5	72.7	72.6	73.0	72.7
C3	75.2	75.0	75.1	75.0	74.7	74.9	74.9	75.0	75.0	75.1	75.4	75.1
C4	68.7	68.6	68.5	68.6	68.5	68.6	68.5	68.5	68.5	68.7	68.6	68.6
C5	74.2	74.1	73.9	74.1	73.6	73.8	73.8	73.8	74.0	73.7	74.0	73.8
C6	72.1	72.1	72.0	72.1	71.9	72.0	71.9	72.3	72.0	72.0	72.2	72.1
C7	64.0	63.9	63.8	63.9	63.6	63.8	63.8	63.8	63.8	63.8	64.0	63.8
^{1}H Chemical shifts[a]												
H2	3.90	3.84	3.89	3.84	3.96	3.90	3.90	3.88	3.90	3.88	4.08	3.90
H3	3.66	3.60	3.62	3.58	3.68	3.63	3.64	3.63	3.65	3.62	3.71	3.64
H4	3.82	3.80	3.81	3.80	3.83	3.80	3.81	3.81	3.82	3.78	3.88	3.80
H5	3.42	3.37	3.40	3.36	3.42	3.39	3.40	3.40	3.40	3.38	3.46	3.40
H6	3.46	3.43	3.44	3.43	3.45	3.43	3.44	3.44	3.45	3.42	3.46	3.43
H7a	3.35	3.30	3.32	3.32	3.33	3.31	3.33	3.32	3.34	3.31	3.34	3.31
H7b	3.54	3.48	3.51	3.51	3.52	3.50	3.52	3.51	3.52	3.51	3.53	3.50
OH2	5.58	5.43	5.48	5.34	5.67	5.58	5.58	5.50	N.D.	N.D.	5.54	N.D.
OH3	4.85	4.75	4.77	4.70	4.84	4.81	4.78	4.78	N.D.	N.D.	4.83	N.D.
OH4	4.42	4.34	4.37	4.30	4.45	4.36	4.34	4.36	N.D.	N.D.	4.36	N.D.
OH5	4.48	4.40	4.44	4.38	4.59	4.41	4.41	4.42	N.D.	N.D.	4.56	N.D.
OH6	4.50	5.46	4.44	4.42	4.58	4.44	4.44	4.45	N.D.	N.D.	4.49	N.D.
OH7	4.36	4.30	4.29	4.27	4.50	4.28	4.29	4.29	N.D.	N.D.	4.33	N.D.
NH1	7.87	7.56	7.80	7.58	8.38	7.77	7.81	7.86	7.96	7.72	8.96	7.94
Coupling constants $^{3}J_{H,H}$												
$J_{2,3}$	6.3	6.4	6.4	6.1	6.3	6.2	6.1	6.3	6.5	5.9	6.7	5.9
$J_{3,4}$	2.4	2.7	2.7	3.2	2.6	3.1	2.9	2.6	2.7	3.4	3.1	3.1
$J_{4,5}$	2.6	2.6	2.6	2.2	2.2	2.1	2.4	2.7	2.5	2.3	2.7	2.5
$J_{5,6}$	7.6	7.4	7.5	8.0	7.8	8.4	7.8	7.3	7.7	7.8	6.5	7.8
$J_{6,7a}$	6.5	6.3	6.0	6.1	6.1	5.3	5.8	6.0	6.0	6.1	4.6	6.0
$J_{6,7b}$	3.9	3.4	3.4	3.3	3.2	3.3	3.3	3.2	3.1	3.2	3.7	3.2
$J_{7a,7bB}$	10.9	10.8	10.7	10.9	11.0	11.0	10.9	11.0	11.0	11.0	10.8	10.9
$J_{2,H2O}$	5.6	6.6	6.5	6.7	6.3	6.3	6.5	6.4	N.D.	N.D.	6.6	N.D.
$J_{3,H3O}$	4.9	4.6	4.4	4.7	4.4	4.2	4.3	4.6	N.D.	N.D.	5.1	N.D.
$J_{4,H4O}$	4.4	6.6	6.5	6.6	6.3	6.4	6.5	6.4	N.D.	N.D.	6.7	N.D.
$J_{5,H5O}$	4.5	5.1	5.1	5.1	5.6	5.1	5.1	5.1	N.D.	N.D.	5.7	N.D.
$J_{6,H6O}$	4.5	5.5	5.0	5.5	5.6	5.4	5.4	5.3	N.D.	N.D.	5.5	N.D.
$J_{7A,H7O}$	4.4	5.8	5.7	5.8	5.6	5.6	5.6	5.8	N.D.	N.D.	5.7	N.D.
$J_{7B,H7O}$	4.4	5.8	5.8	5.8	5.7	5.8	5.8	5.8	N.D.	N.D.	5.8	N.D.
$J_{HN1,8}$	4.7	8.3	5.9	7.8	6.0	5.8	5.7	6.1	5.7	5.7	—	N.D.
^{15}N Chemical shifts[a]												
N1	105.5	135.0	117.3	129.3	95.2	113.5	113.1	117.9	115.0	105.6	125.7	115.9

[a] All the measurements were done in Me_2SO-d_6, using electronic reference.[18]

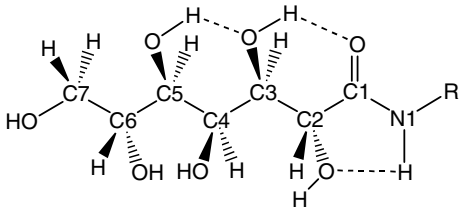

Figure 1. D-Glucoheptonic moiety's conformation of the D-glucoheptonamides **1**–**12** in solution with the intramolecular HB's shown.

determine that the carbon chain conformation of the glucohepton moiety is all-trans. Extra evidence of this conformation is given from the lack of the NOE peak between H2 and H5 in the NOESY spectra (Fig. S1, Supplementary data), it should be present if the conformation was a bent one. Instead of that peak, there is a NOE peak between H3 and H5, which is expected for an all-trans conformation.

This conformation is stabilized by intramolecular hydrogen bonds (HB's): O5–H···O3, O3–H···O1, and N1–H···O2 (Fig. 1). It is important to note that the HB N1–H···O2 is found also in the crystal structures reported here. The formation of these HB's is supported by the chemical shifts at low fields in ^{1}H NMR, of the hydroxyl groups (Table 1), the δ^{1}H for hydroxyl groups OH2 and OH3 in the family of amides are in the ranges 5.34–5.67 and 4.70–4.85 ppm, respectively.

Due to the common conformation of the glucoheptonic moiety in D-glucoheptonamides **1**–**12**, the NMR data (Table 1) show similar values for their ^{1}H and ^{13}C chemical shifts. A closer analysis revealed that the carbonyl group is the most affected functionality by the N-substituent; also, C3 and C5 are affected, this is associated to the inductive effect of the carbonyl group and to the intramolecular HB's formed, as this is the case for H2 and H3.

We also acquired the ^{15}N chemical shifts for the D-glucoheptonamides prepared. The δ^{15}N of the amide groups are shifted to low field with respect to amide **2** (105.5 ppm), as a result of the β effect (Table 1),[9,10] amides **5** (95.2 ppm) and **10** (105.6 ppm) were exceptions. This should be due to hyperconjugation and mesomeric effects.

Table 2. Crystal data and structure refinement parameters

	3	**4**	**5**	**7**	**8**	**9**	**11**
Empirical formula	$C_{11}H_{23}NO_7$	$C_{12}H_{23}NO_7$	$C_{14}H_{21}NO_7$	$C_{10}H_{21}NO_8$	$C_{11}H_{23}NO_8$	$C_{16}H_{32}N_2O_{14}$	$C_{13}H_{20}N_2O_7$
Formula weight	281.30	293.31	315.32	283.28	297.3	476.44	316.31
Crystal system	Triclinic	Triclinic	Triclinic	Monoclinic	Triclinic	Monoclinic	Triclinic
Space group	*P*1	*P*1	*P*1	*P*2(1)	*P*1	*C*2	*P*1
a (Å)	5.8051(9)	4.928(2)	8.913(2)	4.8340(10)	4.8205(16)	35.057(8)	5.6451(15)
b (Å)	12.8964(19)	6.064(3)	5.0967(11)	23.428(5)	6.091(2)	6.0283(13)	5.8286(15)
c (Å)	19.134(3)	12.623(6)	31.892(7)	6.0269(12)	12.496(4)	5.0348(11)	11.571(3)
a (°)	92.297(3)	102.188(8)	90.032(3)	90	85.068(6)	90	90.614(5)
b (°)	98.518(3)	96.009(7)	95.313(3)	90.735(3)	84.864(6)	91.921(4)	99.515(5)
g (°)	101.734(3)	90.713(7)	90.004(3)	90	88.838(6)	90	97.012(5)
V (Å^3)	1383.4(4)	366.5(3)	1442.5(5)	682.5(2)	364.0(2)	1063.4(4)	372.50(17)
Z	4	1	4	2	1	2	1
ρ Calculated (g cm^{-3})	1.351	1.329	1.286	1.378	1.356	1.488	1.410
μ (mm^{-1})	0.112	0.109	0.107	0.119	0.116	0.131	0.115
F(000)	608	158	600	304	160	508	168
θ Range data collection (°)	1.62–25.00	1.66–23.31	1.28–25.00	1.74–25	1.64–23.27	1.16–28.07	1.79–24.99
Index ranges	$-6 \leqslant h \leqslant 6$	$-5 \leqslant h \leqslant 5$	$-10 \leqslant h \leqslant 10$	$-5 \leqslant h \leqslant 6$	$-5 \leqslant h \leqslant 5$	$-45 \leqslant h \leqslant 44$	$-6 \leqslant h \leqslant 6$
	$-9 \leqslant k \leqslant 15$	$-6 \leqslant k \leqslant 6$	$-6 \leqslant k \leqslant 6$	$-27 \leqslant k \leqslant 27$	$-4 \leqslant k \leqslant 6$	$-7 \leqslant k \leqslant 7$	$-6 \leqslant k \leqslant 6$
	$-22 \leqslant l \leqslant 22$	$-13 \leqslant l \leqslant 13$	$-37 \leqslant l \leqslant 37$	$-7 \leqslant l \leqslant 7$	$-13 \leqslant l \leqslant 13$	$-6 \leqslant l \leqslant 6$	$-13 \leqslant l \leqslant 13$
Data collected/unique	7075/4819	2690/1059	13,758/9873	6512/2399	1592/1302	6169/1382	3635/1310
Data [$I > 2\sigma(I)$]	4097	935	3634	2366	1249	805	1003
R(int)	0.0722	0.0636	0.0971	0.0219	0.0163	0.0861	0.0416
% Completeness to θ	99.0	99.4	99.8	99.8	98.7	97.5	99.8
Data/restraints/parameters	4819/3/946	1059/3/225	9873/3/1066	2399/1/243	1302/3/259	1382/1/210	1310/3/260
Goodness-of-fit on F^2	0.978	1.043	0.743	1.150	1.029	0.862	1.116
*R*1 (all data)	0.0524	0.0603	0.1263	0.0361	0.0375	0.0643	0.0626
*R*1 [$I > 2\sigma(I)$]	0.0455	0.0552	0.0686	0.0348	0.0364	0.0342	0.0410
*wR*2 (all data)	0.1049	0.1439	0.1811	0.0782	0.0972	0.0934	0.0788
*wR*2 [$I > 2\sigma(I)$]	0.1008	0.1386	0.1729	0.0775	0.0963	0.0900	0.0717
Extinction coefficient	0.0000(13)	0.02(3)	0.0016(13)	0.000(3)	0.000(16)	0.000(2)	0.000(9)
Weight scheme *W*, where $P = (F_o^2 + 2F_c^2)/3$	$1/[\sigma^2(F_o^2)+(0.0530P)^2]$	$1/[\sigma^2(F_o^2)+(0.1014P)^2]$	$1/[\sigma^2(F_o^2)]+(0.1090P)^2$	$1/[\sigma^2(F_o^2)+(0.0351P)^2+0.0729P]$	$1/[\sigma^2(F_o^2)+(0.0765P)^2]$	$1/[\sigma^2(F_o^2)+(0.0461P)^2+0.1922P]$	$1/[\sigma^2(F_o^2)]$
Largest diff. peak and hole (e Å^{-3})	0.199 −0.230	0.210 −0.197	0.216 −0.301	0.127 −0.134	0.154 −0.169	0.172 −0.139	0.155 −0.176

2.2. Solid state analysis by X-ray diffraction

We were able to crystallize eight of the 12 amides, their crystal data are summarized in Table 2. The glucoheptonic moiety's conformation bore by the amides **4**, **7**–**9**, and **11** was ${}_2G^-$, ${}_3G^-$, ${}_4T$, ${}_5T$ as the reported for amide **2**.[11] This conformation is generated by a double bond rotation, the first one is in the C3–C4 bond to prevent the 1,3-syndiaxial interaction between OH3 and OH5. But, this rotation generates a 1,3-syndiaxial interaction between C5 and OH2, the second rotation about the C2–C3 bond takes place to avoid it. This conformation generated two planes, C1/C2/C3 and C3/C4/C5/C6/C7, with an average interplanar angle of 88° (Fig. S2, Supplementary data).

Amides **4**, **7**, **8**, and **11** are packing in a *head-to-tail* mode which is the same crystal packing as described for amide **2**. The packing can be expressed as a stacking of sheets along a crystallographic axis (*b* axis for amide **7**, and *c* axis for amides **4**, **8**, and **11**) (Fig. S3, Supplementary data).

For amides **4** and **7**, the sheets consist of a 2-D hydrogen bonding (HB)-network, which is formed by two motifs as described for amide **2**. The first motif is an 18-membered ring connected through O1, O2, and O3, which generates the 2-D HB-network (Fig. 2); the second motif are $(OH)_4$ rings [···H–O4···H–O6···H–O7···H–O5···] that are interconnected via intramolecular HB's forming ribbons (Fig. 3). The intramolecular HB's are O4···H–O5, O7···H–O6, and O2···H–N1 (Table 3). The first two HB's depend on the orientation of the hydroxyl groups, but the last one is a common feature along the amides, except for amide **5**, which is substituted with an intermolecular HB (O1···H–N1) vide infra.

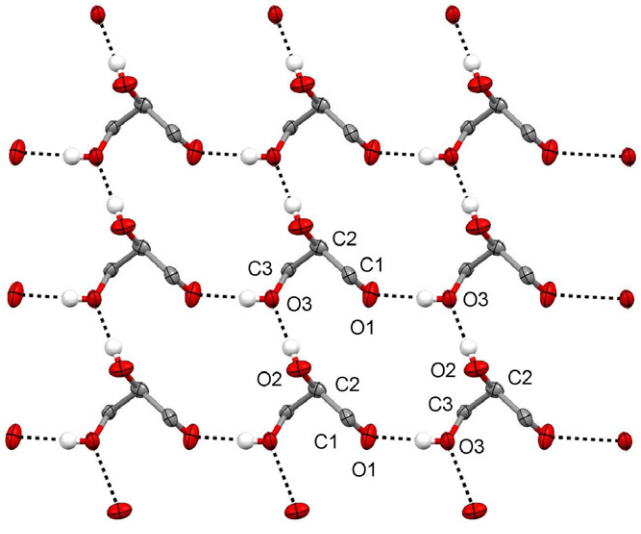

Figure 2. Eighteen-membered ring network for amide **7** as example. View along *b* axis with *c* axis horizontal. For clarity just the atoms C1(O1)–C2(OH2)–C3(OH3) are shown.

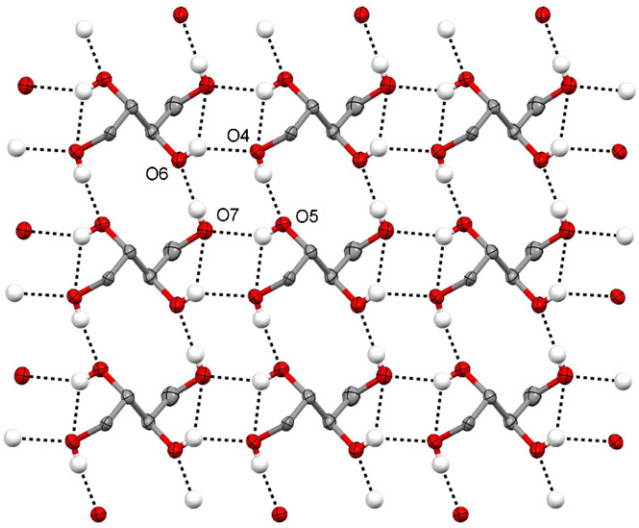

Figure 3. Ribbons formed by the association of the $(OH)_4$ rings [···O7–H···O6–H···O4–H···O5–H···] via intermolecular HB's [O7···H–O6, O4···H–O5] for amide **7** as example. For clarity just the atoms C4(OH4)–C7(OH7) are shown. View along *b* axis with *c* axis horizontal.

Table 3. HB geometry parameters for amide **7**

D–H···A	*d*(D–H)	*d*(H···A)	*d*(D···A)	∠(DHA)
N1–H1N···O2	0.80	2.19	2.586(3)	111
O2–H2O···O3[a]	0.82	1.91	2.732(2)	178
O3–H3O···O1[b]	0.82	1.86	2.679(2)	175
O4–H4O···O5[c]	0.82	1.93	2.742(2)	173
O5–H5O···O4	0.82	2.35	2.754(2)	111
O5–H5O···O7[b]	0.82	2.06	2.780(2)	146
O6–H6O···O4[d]	0.82	2.06	2.763(2)	144
O6–H6O···O7	0.82	2.53	2.847(2)	104
O7–H7O···O6[a]	0.82	1.90	2.722(2)	178

[a] $x+1, y, z$.
[b] $x, y, z+1$.
[c] $x-1, y, z$.
[d] $x, y, z-1$.

In addition to the HB's of the type [O···H–O], there are HB's of the type [O···H–C] in the crystal packing of amide **7**. The oxygens O2, O3, O5, O7, and O8 participate as acceptors; and the carbons C7–C10 as donators with the C···O and C–H···O distances in the ranges 3.39–3.76 and 2.68–3.47 Å, respectively (Table 4). These HB's are important, because they interconnect the sheets, generating a denser packing (Fig. S4, Supplementary data). It is interesting to note that the O8 of amide **7** only participated in HB of type [O···H–C] and did not participate in HB of the type [O···H–O]. The criteria followed to assign the HB [O···H–C] was: *r*(C···O) [3.0–4.0 Å], *r*(H···O) [2.2–3.5 Å], ∠(C–H···O) [90–150°], and [60–150°] for the angles (CH···O–H), (CH···O–C), and (H···O···H).[12]

For amide **8**, the [O···H–O] HB and the motifs found are the same as described above with however a new one

Table 4. [O···H–C] HB geometry parameters of amide **7**

C–H···O	*d*(C···O)	*d*(H···O)	∠(C–H···O)	∠(H···O–H)[f]	∠(H···O–C)	∠(H···O···H)[g]
C7–H7A···O8[a]	3.617	3.215	107.8	120.7	108.3	—
C8–H8A···O2[b]	3.711	3.226	111.3	90.1	92.8	68.4
C8–H8A···O8[b]	3.755	3.462	99.6	100.2	92.8	119.9
C8–H8B···O8[b]	3.755	3.377	108.4	97.3	116.7	102.1
C9–H9A···O2[c]	3.714	2.756	157.7	116.0	112.2	74.8
C9–H9A···O3[c]	3.395	2.683	127.2	76.2	115.0	94.4
C10–H10A···O7[d]	3.398	3.271	89.4	73.8	119.0	80.8
C10–H10B···O5[e]	3.634	2.802	149.2	75.8	134.0	91.0
C10–H10B···O7[d]	3.398	2.928	112.7	98.5	98.5	63.3

[a] $-x+1,\ y+1/2,\ -z+1$.
[b] $x+1,\ y,\ z$.
[c] $x,\ y,\ z+1$.
[d] $-x,\ y-1/2,\ -z+2$.
[e] $-x,\ y-1/2,\ -z+1$.
[f] For oxygen O8, we took the methyl group as the hydrogen to measure the angle.
[g] The (H···O···H) angle for C7–H7A···O8 are the listed for C8–H8A···O8 and C8–H8B···O8.

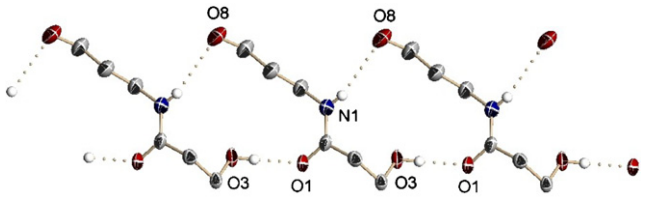

Figure 4. Partial view of the 1-D HB-network formed in the crystal of amide **8**. This network is orthogonal to the 2-D HB-network generated by the 18-membered ring. Some atoms were omitted for clarity. View along axis *a* with axis *b* horizontal.

in which O-8 participates in the HB-network. The new pattern formed is a 14-membered macrocycle that extends along the **b** axis and is orthogonal to the HB-network made by the 18-membered rings. It is connected by two intermolecular HB's through N1–H···O8 [2.61 Å] and O3–H···O1 [1.83 Å] (Fig. 4). There are also HB of the type [O···H–C] as in the case of amide **7** (Fig. S5, Supplementary data). The [O···H–C] HB acceptors are O1–O3, O5, O7, and O8; with C2, C7, and C9–C11 as HB donators. The distances C···O and C–H···O are in the ranges 3.61–3.98 and 2.70–3.20 Å, respectively (Table 5).

The presence of the aromatic ring in amide **11** changes the orientation of the hydroxyl groups in the glucoheptonic moiety, and because of this, the patterns also change. A closer analysis reveals that the $(OH)_4$ rings are different compared to those formed by the amides previously described. The interconnectivity for the ring in the present packing is [···H–O4···H–O5···H–O7···H–O6···], while the usual interconnectivity is [···H–O4···H–O6···H–O7···H–O5···] (Table 6). The change in orientation of the OH groups also prevents the formation of ribbons from the association of $(OH)_4$ rings because the intramolecular HB's that generate them are not present. The 18-membered ring previously described is replaced by a 22-membered ring, with the participation of the amine nitrogen in it, which consists of two of the following HB's: N2–H···O2 [2.11 Å], O2–H···O1 [1.85 Å] (Table 6). In addition, this ring is divided by another HB, O3–H···N2 [2.38 Å] in two rings: one 12-membered ring and other 18-membered ring (Fig. 5). The aromatic ring participates in

Table 5. [O···H–C] HB geometry parameters of amide **8**

C–H···O	*d*(C···O)	*d*(H···O)	∠(C–H···O)	∠(H···O–H)[g]	∠(H···O–C)	∠(H···O···H)
C2–H2···O1[a]	3.943	3.19	134.0	—	96.5	108.1
C7–H7···O8[b]	3.974	3.14	162.5	88.2	88.7	147.8
C9–H9A···O2[c]	3.647	2.70	160.9	112.9	118.8	75.3
C9–H9A···O3[c]	3.538	2.86	126.6	79.2	112.8	94.5
C10–H10A···O2[d]	3.855	3.02	154.1	75.3	170.2	91.3
C11–H11A···O5[e]	3.671	3.13	117.2	72.7	155.0	72.3
C11–H11A···O7[f]	3.614	2.78	146.4	89.6	116.9	74.8

[a] $x-1,\ y,\ z$.
[b] $x,\ y,\ z+1$.
[c] $x,\ y-1,\ z$.
[d] $x+1,\ y-1,\ z$.
[e] $x+1,\ y-1,\ z-1$.
[f] $x+1,\ y,\ z-1$.
[g] For oxygen O8, we took the methyl group as the hydrogen to measure the angle.

Table 6. HB geometry parameters for amide **11**

D–H···A	*d*(D–H)	*d*(H···A)	*d*(D···A)	∠(DHA)
N1–H1N···O2	0.85	2.13	2.551(5)	110
N2–H2AN···N1	1.05(11)	2.38(10)	2.790(9)	102(6)
N2–H(2BN)···O2[a]	0.85(10)	2.11(10)	2.925(7)	161(9)
O2–H2O···O1[b]	0.82	1.85	2.668(4)	173.5
O3–H3O···N2[b]	0.82	2.38	3.174(9)	163.9
O4–H4O···O6[b]	0.82	2.00	2.810(4)	171.1
O5–H5O···O4[c]	0.82	1.95	2.759(4)	167.9
O6–H6O···O7[d]	0.82	1.96	2.754(4)	163.4
O7–H7O···O5[e]	0.82	1.95	2.735(4)	159.5

[a] $x+1, y+1, z$.
[b] $x, y-1, z$.
[c] $x-1, y, z$.
[d] $x+1, y, z$.
[e] $x, y+1, z$.

the stabilization of the crystal lattice by means of N–H···π interactions through the amide. This interaction generates infinite chains along axis *b* (Fig. 6). The distance from this proton to the nearest carbon is 2.845 Å and to the aromatic mean plane it is 2.791 Å. Both distances are shorter than the addition of the van der Waals radii of carbon and proton (2.9 Å).

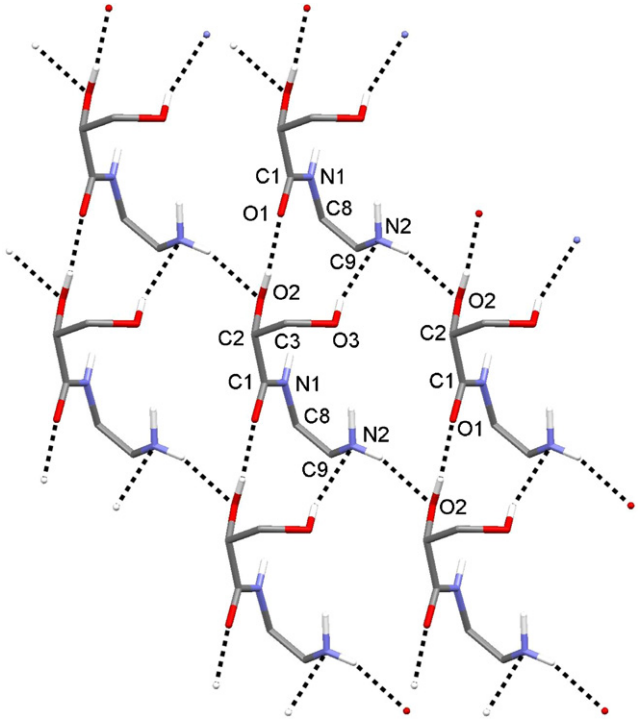

Figure 5. View along *c* axis with *a* axis horizontal of the crystal packing of amide **12**. Section of the 2-D HB-network generated by the 12- and 18-membered rings with the participation of N2 is shown. Some atoms were omitted for clarity.

For amide **9**, we found the same [O···H–O] HB patterns as for amides **2**, **4**, and **7**, but differing in the packing due to the ethylene bridge, which causes the molecules to arrange in a *tail-to-tail* mode (bilayer mode). There are also two [O···H–C] HB: C7–H8···O7 (2.63 Å) and C8–H10···O3 (2.83 Å) (Table 7), which are responsible for the dense packing (Fig. 7).

For amide **3**, we found four conformers in the unit cell (A, B, C, and D), the conformers A and D show disorder in the isobutyl group. These conformers differ essentially in the torsion angle C1–N1–C8–C9 [A: 125.2(7), 77.1(15); B: −94.5(5); C: 155.3(5); D: 115(3), 156.4(7)]. The rotation about the bond N1–C8 is required to accommodate the bulky isobutyl group. The conformation of this amide is also a double bend; however, the carbon chain conformation changed to ${}_2G^+$, ${}_3G^+$, ${}_4T$, ${}_5T$. This change is due to the presence of the isobutyl group. The packing can be described as a stacking of shifted monolayers (one for each conformer); within each monolayer, the arrangement of the molecules alternates between *head-to-tail* and *tail-to head* modes through the layer-stacking (Fig. 8). An interesting feature arises from this packing, that is a pseudo-hexagonal arrangement (Fig. 9), and due to this arrangement, the hydroxyl groups adopt an orientation that allows only one intramolecular hydrogen bond of medium strength N1–H···O2 [2.08 Å]. Note that N1 does not take part in the intermolecular HB-network. This network is formed by 27 intermolecular HB's of medium strength (the distance from donor to acceptor is within 2.5–3.2 Å),[13] (Table S5, Supplementary data).

In the case of amide **5**, there are four conformers in the asymmetric unit, which are slightly different and present disorder in the orientation of the aromatic ring. The position of the second ring is generated by rotation of the C8–C9 bond by 75.5°. The glucoheptonic moiety's conformation is ${}_2T$, ${}_3T$, ${}_4T$, ${}_5T$, this change is due to the lack of a group on the aromatic ring that can form HB as in the case of amide **12**. Because of that, the hydrophobic character of the aryl group is not diminished. This conformation should be similar to the one deter-

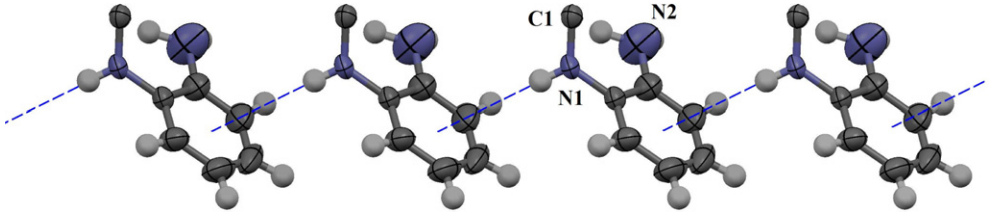

Figure 6. View of the chain generated due to N–H···π interactions in amide **12** along the *b* axis. Some atoms were omitted for clarity.

Table 7. [O···H–C] HB geometry parameters of amide **9**

C–H···O	*d*(C···O)	*d*(H···O)	∠(C–H···O)	∠(H···O–H)	∠(H···O–C)	∠(H···O···H)
C7–H8···O7[a]	3.570	2.634	145.83	101.80	93.51	66.36
C8–H10···O3[a]	3.577	2.831	133.88	59.90	117.37	101.25

[a] $-x+1/2,\ y+1/2,\ -z+1$.

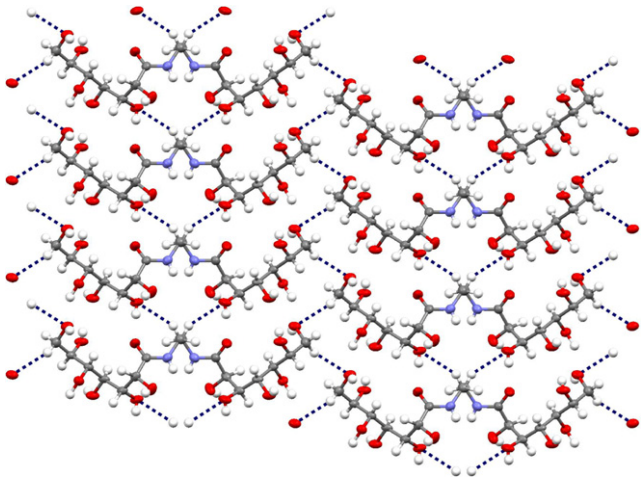

Figure 7. Bilayer packing of amide **9**. Dotted lines are the [O···H–C] HB. View along the *c* axis with *a* horizontal.

mined in solution for all the amides, although the orientation of the hydroxyl groups may not be the same. We found that the crystal packing is formed by bilayers. The conformers display an intramolecular HB-that connects one conformer with the other, via the terminal hydroxyl group from one layer to the other (O7–H···O7) [2.10 and 1.89 Å due to the two conformers in each layer]. In this interaction, the donor atom belongs to one conformer and the acceptor atom is from the other one (Fig. 10). There are π–π interactions, the distances between the planes of the aromatic rings in the stacking mode are 1.81 and 4.87 Å, and for the herringbone mode, the distance between the edge and the plane of the aromatic ring is 3.02 Å (Fig. 11).

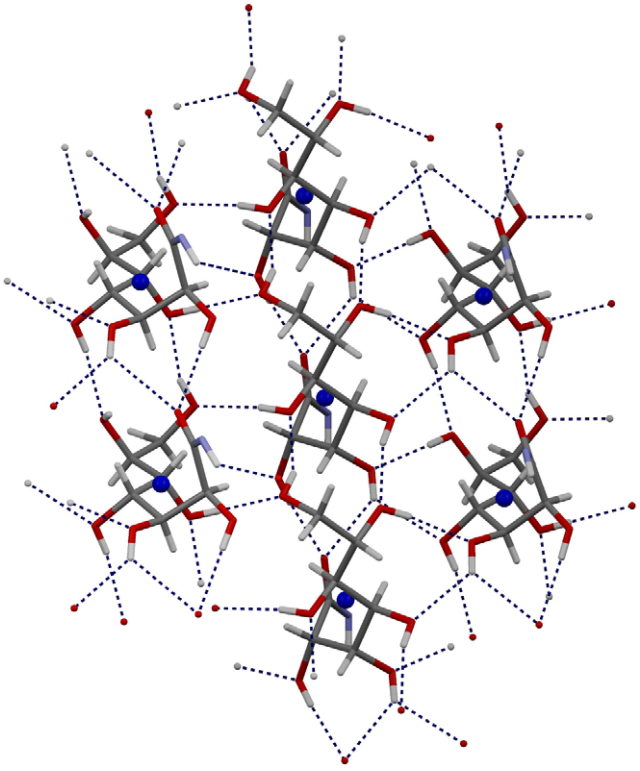

Figure 9. Pseudohexagonal packing adopted by amide **3**, where the HB-network is shown. The dots are the centroids of the hydroxyl groups of each glucoheptonamide moiety. Some atoms were omitted for clarity.

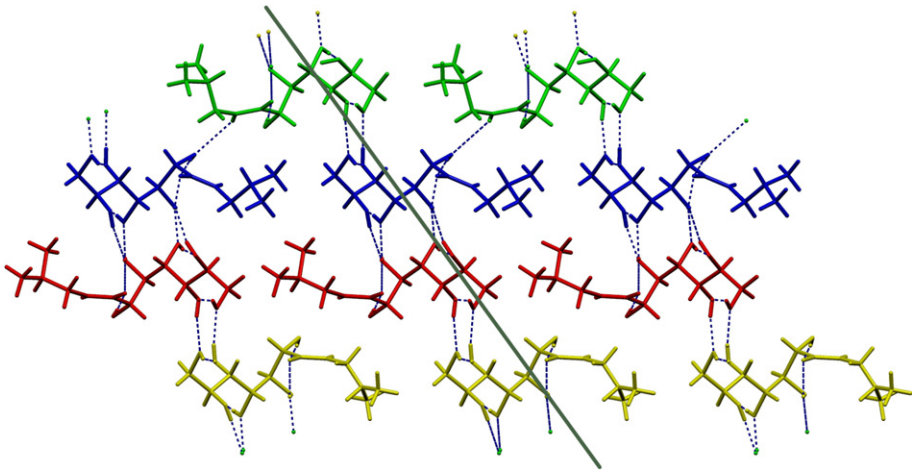

Figure 8. Layer stacking in the crystal packing of **3**. Each layer is formed with a different conformer as is shown by the colors. The line is the plane in which the pseudohexagonal packing is found (see text and Fig. 9).

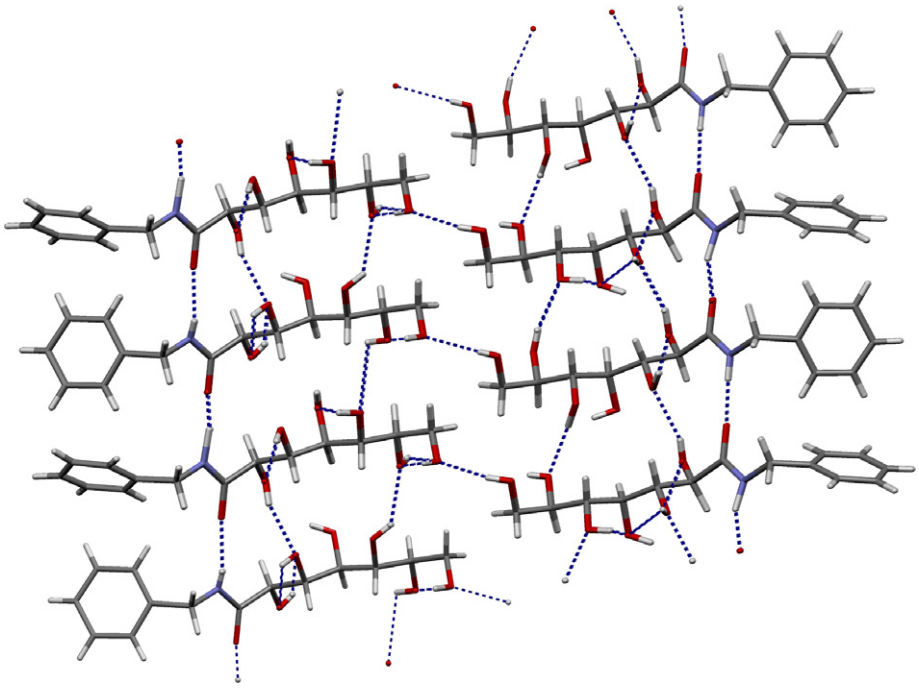

Figure 10. View of the crystal packing of amide **5**. Here are shown the intermolecular HB's only. Note the HB that joins the bilayer.

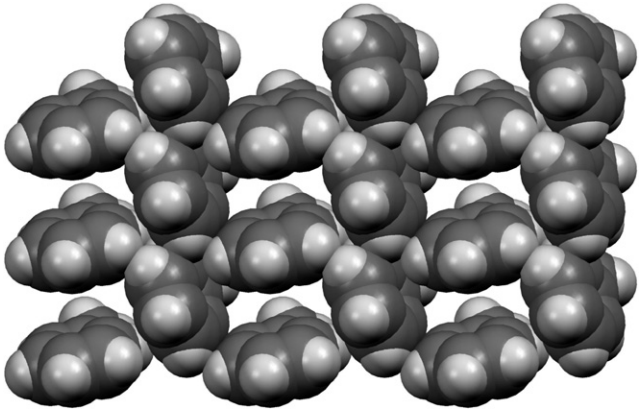

Figure 11. View of the aromatic rings' packing for amide **5**.

3. Conclusions

The preferred conformation in Me_2SO-solution ($_2T$, $_3T$, $_4T$, $_5T$) of the studied aldonamides does not depend on the nature of the N-substituent as shown from the NMR data (Table 1). In addition, we conclude that just the N1–C1–C2–C3 fragment is affected by the N-substituent.

On the other hand, the packing of these compounds in solid state strongly depends on the nature of the N-substituent. In the case of sterically demanding groups such as isobutyl, benzyl and cyclopentyl, a spatial disorder is observed, because of the lack of HB acceptor and/or donator groups.

We have found three different crystal packings and conformations along the amides. Amides **2**, **4**, **7**, **8**, and **11** arrange in a *head-to-tail* mode; amides **5** and **9** pack in a *head-to-head* mode (bilayer), while amide **3** shows a pseudohexagonal packing. The three conformations found are $_2G^-$, $_3G^-$, $_4T$, $_5T$ for amides **2**, **4**, **7**, **8**, **9**, and **11**; $_2G^+$, $_3G^+$, $_4T$, $_5T$ for amide **3**; and $_2T$, $_3T$, $_4T$, $_5T$ for amide **5**, indicating that the glucoheptonic moiety's conformation changes with the volume of the N-substituent. Only amide **5** shows a conformation such as found in Me_2SO solution for the amides, however, the hydroxyl groups' orientation may be not the same.

The [O···H–O] HB motifs are very important in the stability of the crystal lattice, as is shown by the presence of the 18-membered ring network and the $(OH)_4$ rings in the crystal packing of amides **2**, **4**, **7**, **8**, and **9**. When they are not formed as in the case of amides **3** and **5**, the lack is supplied by more complicated HB systems. The named weak HB's as C–H···O and X–H···π (X = N, C) are also important in the crystal packing, they avoid the disordered structures and allow more dense packings.

4. Experimental

Infrared spectra were recorded in KBr using a Bruker Vector 22 instrument. Optical rotations were measured in a Perkin Elmer 341 Polarimeter. Elemental Analyses (C, H, and N) were performed with a Vario EL III Elemental Analyzer. Melting points were measured with a Büchi apparatus and are uncorrected. NMR spectra were acquired with a Varian UnityInova 400 MHz

spectrometer. The X-ray diffraction analyses were performed with a Bruker-A xs Apex diffractometer.

4.1. Materials

D-*glycero*-D-*gulo*-Heptono-1,4-lactone was purchased from Aldrich and used without further purification. All amines used are commercially available.

4.2. General procedure (GP) for the syntheses of the amides

D-*glycero*-D-*gulo*-Heptono-1,4-lactone (1.00 g, 4.80 mmol) was suspended in warm EtOH (50 mL) and dissolved with a few drops of water. The corresponding amine (5.28 mmol) was added, then the soln was refluxed for 1 h, and it was slowly cooled to room temperature.

4.3. *N*-Methyl-D-*glycero*-D-*gulo*-heptonamide (1)

D-*glycero*-D-*gulo*-Heptono-1,4-lactone (1.00 g, 4.80 mmol) was suspended in EtOH (10 mL) in a 50 mL reactor, the methylamine (0.16 g, 5.28 mmol) and a few drops of water were added. The reactor was closed and heated in an oil bath with a magnetic stirrer at 100 °C for 1 h, and then it was cooled slowly to room temperature. 0.64 g (55.8%); mp 168–170 °C; $[\alpha]_D^{20}$ +8.0 (*c* 1.4, water); IR (KBr); *v* 1619 cm^{-1} (amide); ^1H NMR (Me_2SO, 400 MHz): δ 2.59 (d, 3H, $J_{8,N}$ 4.7 Hz, H8); ^{13}C NMR (Me_2SO, 400 MHz): δ 26.2 (1C, C8). Anal. Calcd for $C_8H_{17}NO_7$: C, 40.17; H, 7.16; N, 5.86; O, 46.82. Found: C, 39.67; H, 7.91; N, 5.84; O, 47.45.

4.4. *N*-Isopropyl-D-*glycero*-D-*gulo*-heptonamide (2)

Via GP from isopropylamine (0.31 g); recrystallized from water/acetone; 0.60 g (46.8%); mp 161–162 °C; $[\alpha]_D^{20}$ +8.1 (*c* 1.3, water); IR (KBr): *v* 1656 and 1548 cm^{-1} (amide); ^1H NMR (Me_2SO, 400 MHz): δ 3.83 (m, 1H, $J_{8,HN1}$ 4.7, $J_{8,9}$ 6.4, $J_{8,10}$ 6.6 Hz, H8), 0.99 (d, 6H, H9, H10); ^{13}C NMR (Me_2SO, 400 MHz): δ 40.7 (1C, C8), 22.9 (2C, C9, C10). Anal. Calcd for $C_{10}H_{21}NO_7$: C, 44.4; H, 7.92; N, 5.24; O, 41.90. Found: C, 44.92; H, 7.96; N, 5.27; O, 41.85.

4.5. *N*-Isobutyl-D-*glycero*-D-*gulo*-heptonamide (3)

Via GP from isobutylamine (0.39 g); recrystallization from EtOH/water gave needles; 0.94 g (69.8%); mp 145–147 °C; $[\alpha]_D^{20}$ +12.8 (*c* 1.4, water); IR (KBr): *v* 1645 and 1546 cm^{-1} (amide); ^1H NMR (Me_2SO, 400 MHz): δ 2.87 (dd, 1H, $J_{8,HN1}$ 5.9, $J_{8,9}$ 7.2 Hz, H8), 1.68 (dq, 1H, $J_{9,10}$ 6.7 Hz, H9), 0.78 (d, 6H, H10, H11); ^{13}C NMR (Me_2SO, 400 MHz): δ 46.2 (1C, C8), 28.3 (1C, C9), 20.5 (2C, C10, C11). Anal. Calcd for $C_{11}H_{23}NO_7$: C, 46.97; H, 8.24; N, 4.98; O, 39.81. Found: C, 46.69; H, 8.28; N, 4.91; O, 40.12.

4.6. *N*-Cyclopentyl-D-*glycero*-D-*gulo*-heptonamide (4)

Via GP from cyclopentylamine (0.45 g); recrystallization from EtOH gave trigonal prismatic crystals; 0.94 g (56.6%); mp 156–160 °C; $[\alpha]_D^{20}$ +5.1 (*c* 1.6, water); IR (KBr): *v* 1657 and 1542 cm^{-1} (amide); ^1H NMR (Me_2SO, 400 MHz): δ 3.96 (m, 1H, $J_{8,HN1}$ 7.8 Hz H8), 1.71 (m, 2H, H9A, H12A), 1.57 (m, 2H, H10A, H11A), 1.40 (m, 2H, H10B, H11B), 1.35 (m, 2H, H9B, H12B); ^{13}C NMR (Me_2SO, 400 MHz): δ 50.6 (1C, C8), 32.7 (2C, C9, C12), 24.0 (2C, C10, C11). Anal. Calcd for $C_{12}H_{23}NO_7$: C, 49.14; H, 7.90; N, 4.78; O, 38.18. Found: C, 48.95; H, 7.86; N, 4.78; O, 38.41.

4.7. *N*-Benzyl-D-*glycero*-D-*gulo*-heptonamide (5)

Via GP from benzylamine (0.56 g); 1.07 g (71.0%); mp 170–172 °C; $[\alpha]_D^{20}$ +12.4 (*c* 1.5, water); IR (KBr): *v* 1650 and 1541 cm^{-1} (amide); ^1H NMR (Me_2SO, 400 MHz): δ 7.25 (m, 2H, H11, H13), 7.23 (m, 1H, H12), 7.17 (m, 2H, H10, H14), 4.32 (dd, 1H, $J_{8A,HN1}$ 6.0, $J_{8A,8B}$ 15.3 Hz, H8A), 4.27 (dd, 1H, H8B); ^{13}C NMR (Me_2SO, 400 MHz): δ 139.5 (1C, C9), 128.6 (2C, C11, C13), 127.5 (1C, C12), 127.1 (2C, C10, C14), 42.2 (1C, C8). Anal. Calcd for $C_{14}H_{21}NO_7$: C, 53.33; H, 6.71; N, 4.44; O, 35.52. Found: C, 53.88; H, 6.87; N, 4.34; O, 34.91.

4.8. *N*-(2-Hydroxyethyl)-D-*glycero*-D-*gulo*-heptonamide (6)

Via GP from 2-hydroxyethylamine (0.32 g); 1.17 g (90.7%); mp 127–130 °C; $[\alpha]_D^{20}$ +11.5 (*c* 1.4, H_2O); IR (KBr): *v* 1655 and 1552 cm^{-1} (amide); ^1H NMR (Me_2SO, 400 MHz): δ 4.66 (d, 1H, $J_{HO8,9}$ 5.6 Hz, HO8), 3.36 (dt, 2H, $J_{9,8}$ 6.2 Hz, H9), 3.12 (dt, 2H, $J_{8,HN1}$ 5.8 Hz, H8); ^{13}C NMR (Me_2SO, 400 MHz): δ 60.1 (1C, C9), 41.6 (1C, C8). Anal. Calcd for $C_9H_{19}NO_8$: C, 40.15; H, 7.11; N, 5.20; O, 47.54. Found: C, 39.65; H, 7.85; N, 5.18; O, 48.12.

4.9. *N*-(2-Methoxyethyl)-D-*glycero*-D-*gulo*-heptonamide (7)

Via GP from 2-methoxyethylamine (0.40 g); 0.93 g (68.7%); mp 109–112 °C; $[\alpha]_D^{20}$ +12 (*c* 1.4, H_2O); IR (KBr): *v* 1652 and 1547 cm^{-1} (amide); ^1H NMR (Me_2SO, 400 MHz): δ 3.32 (m, 2H, H9), 3.22 (m, 2H, $J_{8,HN1}$ 5.7 Hz, H8), 3.20 (s, 3H, H10); ^{13}C NMR (Me_2SO, 400 MHz): δ 70.8 (1C, C9), 58.4 (1C, C10), 38.5 (1C, C8). Anal. Calcd for $C_9H_{19}NO_8$: C, 42.40; H, 7.47; N, 4.94; O, 45.18. Found: C, 42.02; H, 7.47; N, 4.93; O, 45.58.

4.10. *N*-(3-Methoxypropyl)-D-*glycero*-D-*gulo*-heptonamide (8)

Via GP from 3-methoxypropylamine (0.47 g); 0.89 g (62.4%); recrystallization from water/acetone; mp 106–110 °C; $[\alpha]_D^{20}$ +11.2 (*c* 1.4, water); IR (KBr): *v* 1650 and 1559 cm^{-1} (amide); ^1H NMR (Me_2SO, 400 MHz): δ 3.28 (t, 2H, $J_{10,9}$ 6.4 Hz, H10), 3.17 (s, 3H, H11), 3.09 (dt, 2H, $J_{8,9}$ 7.0, $J_{8,HN1}$ 6.1 Hz, H8), 1.61 (tt, 2H, H9); ^{13}C NMR (Me_2SO, 400 MHz): δ 70.3 (1C, C10), 58.3 (1C, C11), 36.2 (1C, C8), 29.5 (1C, C9). Anal. Calcd for $C_{11}H_{23}NO_8 \cdot H_2O$: C, 41.90; H, 7.99; N, 4.44; O, 45.67. Found: C, 42.35; H, 7.97; N, 4.52; O, 45.16.

4.11. 1,2-Ethylen-bis(D-*glycero*-D-*gulo*-heptonamide) (9)

Via GP from 1,2-ethylendiamine (0.32 g); 0.92 g (80.4%). Needle-shaped crystals were obtained from water/MeOH. Mp 187–189 °C; $[\alpha]_D^{20}$ +14 (*c* 1.4, water); IR (KBr): *v* 1658 and 1546 cm^{-1} (amide); ^1H NMR (Me_2SO, 400 MHz): δ 3.14 (s, 4H, $J_{8,HN1}$ 5.7 Hz, H8, H8′); ^{13}C NMR (Me_2SO, 400 MHz): δ 38.8 (2C, C8, C8′). Anal. Calcd for $C_{16}H_{32}N_2O_{14} \cdot 2H_2O$: C, 37.50; H, 7.08; N, 5.47; O, 49.95. Found: C, 37.69; H, 7.03; N, 5.63; O, 49.65.

4.12. *N*-(*N*′,*N*′-Dimethyl-2-aminoethyl)-D-*glycero*-D-*gulo*-heptonamide (10)

Via GP from *N*,*N*-dimethylethylenediamine (0.46 g); 0.92 g (85.0%); mp 121–123 °C; $[\alpha]_D^{20}$ +12.3 (*c* 1.4, water). ^1H NMR (Me_2SO, 400 MHz): δ 3.12 (dt, 2H, $J_{8,HN1}$ 5.7, $J_{8,9}$ 6.6 Hz, H8), 2.24 (t, 2H, H9), 2.24 (t, 2H, H9), 2.07 (s, 6H, H10); ^{13}C NMR (Me_2SO, 400 MHz): δ 58.4 (1C, C9), 45.6 (2C, C10), 36.7 (1C, C8). Anal. Calcd for $C_{11}H_{24}N_2O_7$: C, 44.59; H, 8.16; N, 9.45; O, 37.80. Found: C, 43.98; H, 9.06; N, 9.40; O, 38.28.

4.13. *N*-(2-Aminophenyl)-D-*glycero*-D-*gulo*-heptonamide (11)

D-*glycero*-D-*gulo*-Heptono-1,4-lactone (1.00 g, 4.80 mmol) was suspended in EtOH (13 mL) in a 50 mL reactor and the 2-phenylendiamine (4.14 g, 38.3 mmol) and five drops of water were added. The reactor was closed and heated in an oil bath with a magnetic stirrer at 100 °C for 3 h, then cooled to room temperature. Acetone was added to the reaction crude and crystals were obtained. 1.03 g (67.8%); mp 163–165 °C; $[\alpha]_D^{20}$ +18.5 (*c* 1.3, water); IR (KBr): *v* 1665 and 1525 cm^{-1} (amide); ^1H NMR (Me_2SO, 400 MHz): δ 7.09 (dd, 1H, $J_{13,12}$ 7.9, $J_{13,11}$ 1.7 Hz, H13), 6.87 (dd, 1H, $J_{11,10}$ 8.1, $J_{11,12}$ 7.2 Hz, H11), 6.66 (dd, 1H, $J_{10,12}$ 1.5 Hz, H10), 6.49 (ddd, 1H, H12), 4.85 (s, 2H, HN2). ^{13}C NMR (Me_2SO, 400 MHz): δ 143.3 (1C, C9), 126.8 (1C, C11), 126.6 (1C, C13), 123.5 (1C, C8), 116.6 (1C, C12), 116.1 (1C, C10). ^{15}N NMR (Me_2SO, 400 MHz) δ 58.2 (1N, N2). Anal. Calcd for $C_{13}H_{20}N_2O_7$: C, 49.36; H, 6.37; N, 8.86; O, 35.41. Found: C, 48.93; H, 6.29; N, 8.84; O, 35.94.

4.14. *N*-(3,6-Diaza-hexyl)-D-*glycero*-D-*gulo*-heptonamide (12)

Via GP from bis(2-aminoethyl)amine (0.54 g); the product was obtained as oil, 0.60 g (40%). $[\alpha]_D^{20}$ +9.0 (*c* 1.5, water); IR (KBr): *v* 1656 and 1544 cm^{-1} (amide); ^1H NMR (Me_2SO, 400 MHz): δ 3.12 (t, 2H, $J_{8A,9}$ 5.1, $J_{8B,9}$ 6.6 Hz, H8A, H8B), 2.52 (t, 2H, $J_{11,10}$ 5.7 Hz, H11), 2.51 (dd, 2H, H9), 2.44 (d, 1H, H10). ^{13}C NMR (Me_2SO, 400 MHz): δ 52.2 (1C, C10), 48.8 (1C, C9), 41.6 (1C, C11), 38.7 (1C, C8). ^{15}N NMR (Me_2SO, 400 MHz) δ 104.6 (1N, N2), 66.1 (1N, N3). Anal. Calcd for $C_{11}H_{25}N_3O_7$: C, 42.44; H, 8.09; N, 13.50; O, 35.97. Found: C, 41.91; H, 8.93; N, 13.45; O, 36.45.

4.15. X-ray crystallographic analyses of amides

All X-ray diffraction data were measured on a *Bruker-Axs Apex* diffractometer using monochromatic Mo Kα radiation ($\lambda = 0.71073$ Å) at 293 K. Structures were determined by direct methods and refined by full-matrix least-squares based on F^2. Hydrogen atoms were obtained from difference Fourier maps. Data collection: SMART,[14] cell refinement: SAINT;[14] data reduction: SAINT; program used to solve structure: SHELXS97;[15] program used to refine structure: SHELXL97;[16] software used to prepare material for publication: SHELXTL[14] and Mercury[17]. The weighted *R*-factor *wR* and goodness of fit *S* are based on F^2, conventional *R*-factors *R* are based on *F*, with *F* set to zero for negative F^2. The threshold expression of $F^2 > 2\sigma(F^2)$ is used only for calculating *R*-factors [$I > 2\sigma(I)$], etc. and is not relevant to the choice of reflections for refinement.

Acknowledgments

We thank Dr. Herbert Höpfl for helpful discussions and Dr. Margarita Tlahuextl for the measurement of optical rotations. Funding provided by the Consejo Nacional de Ciencia y Tecnología (CONACyT) under grant 3562P-E and scholarship 165770 is gratefully acknowledged.

Supplementary data

Tables of the HB geometric parameters are included as Supplementary data. Complete structural data under entries CCDC 297251 for **4**, CCDC 297252 for **8**, CCDC 297253 for **6**, CCDC 297254 for **12**, CCDC 297255 for **9**, CCDC 297256 for **10**, and CCDC 297257 for **5** have

been deposited at the Cambridge Crystallographic Data Centre. They can be obtained free of charge via www.ccdc.cam.ac.uk/conts/retrieving.html (or from the CCDC, 12 Union Road, Cambridge CB2 1EZ, UK; fax: +44 1223 336033, e-mail: deposit@ccdc.cam.ac.uk). Supplementary data associated with this article can be found, in the online version, at doi:10.1016/j.carres.2006.11.020.

References

1. Au, V.; Harirchian, B. EP Patent 0,550,106, 1993. CAN 120:11002.
2. Dubois, G. E.; Yalpani, M.; Owens, W. H.; Stevens, S.Y.; Roy, G. WO Patent 9,206,601, 1992. CAN 118:39336.
3. Rieckert, H.; Michel, K.-H.; Zwinselman, J. U.S. Patent 5,952,274, 1997. CAN 128:194574.
4. Kyely, D. E.; Chen, L.; Lin, T.-H. *J. Am. Chem. Soc.* **1994**, *116*, 571–578.
5. Estroff, L. A.; Hamilton, A. D. *Chem. Rev.* **2004**, *104*, 1201–1218; Bhattacharya, S.; Acharya, S. N. G. *Chem. Mater.* **1999**, *11*, 3504–3511; Hafkamp, R. J. H.; Feiters, M. C.; Nolte, R. J. M. *J. Org. Chem.* **1999**, *64*, 412–426.
6. Horton, D.; Varela, O. *Carbohydr. Res.* **1998**, *308*, 85–91.
7. Angyal, S. J.; Le Fur, R. *J. Org. Chem.* **1989**, *54*, 1927–1931.
8. DOHHIR, Tinant, B.; Declercq, J. P.; Van Meerssche, M. *Acta Crystallogr., Sect. C* **1986**, *42*, 579–581; YUXDEA, YUXDAW, Andre, C.; Luger, P.; Bach, R.; Fuhrhop, J.-H. *Carbohydr. Res.* **1995**, *266*, 15–35; PARKEY, Andre, C.; Luger, P.; Svenson, S.; Fuhrhop, J.-H. *Carbohydr. Res.* **1992**, *230*, 31–40; HAHXOD, Andre, C.; Luger, P.; Svenson, S.; Fuhrhop, J.-H. *Carbohydr. Res.* **1993**, *240*, 47–56; CEGLCA01, Sindt, A. C.; Mackay, M. F. *Acta Crystallogr., Sect. B* **1977**, *33*, 2659–2662; DAYVUU, DAYWAB, Darbon-Meyssonnier, N.; Oddon, Y.; Decoster, E.; Pavia, A. A.; Pepe, G.; Reboul, J. P. *Acta Crystallogr., Sect. C* **1985**, *41*, 1324–1327; CIBWIT, Darbon, N.; Oddon, Y.; Lacombe, J. M.; Decoster, E.; Pavia, A. A.; Reboul, J. P. *Acta Crystallogr., Sect. C* **1984**, *40*, 1105–1107; LIHGIS, Andre, C.; Luger, P.; Nehmzow, D.; Fuhrhop, J.-H. *Carbohydr. Res.* **1994**, *261*, 1–11; FATXUT, Oddon, Y.; Darbon-Meyssonnier, N.; Reboul, J. P.; Pepe, G.; Decoster, E.; Pavia, A. A. *Acta Crystallogr., Sect. C* **1986**, *42*, 1764–1766; FAKGAZ01, FAKGIH10, Muller-Fahrnow, A.; Hilgenfeld, R.; Hesse, H.; Saenger, W.; Pfannemuller, B. *Carbohydr. Res.* **1988**, *176*, 165–174; FAKFUS, FAKGED, FAKGON, Zabel, V.; Muller-Fahrnow, A.; Hilgenfeld, R.; Saenger, W.; Pfannemuller, B.; Enkelmann, V.; Welte, W. *Chem. Phys. Lipids* **1986**, *39*, 313–327; PIMFAS, Muller-Fahrnow, A.; Saenger, W.; Fritsch, D.; Schnieder, P.; Fuhrhop, J.-H. *Carbohydr. Res.* **1993**, *242*, 11–20; JIJXEF, Jeffery, G. A.; Maluszynska, H. *Carbohydr. Res.* **1990**, *207*, 211–219; ZOSSAB, Andre, C.; Luger, P.; Gutberlet, T.; Vollhardt, D.; Fuhrhop, J.-H. *Carbohydr. Res.* **1995**, *272*, 129–140.
9. Witanowski, M.; Stefaniak, L.; Webb, G. A. *Annu. Rep. NMR Spectrosc.* **1981**, *11B*, 1–486.
10. Witanowski, M.; Stefaniak, L.; Webb, G. A. *Annu. Rep. NMR Spectrosc.* **1988**, *18*, 1–754.
11. Metta-Magaña, A. J.; Tlahuext, H.; Reyes-Martínez, R. *Acta Crystallogr., Sect. E* **2004**, *60*, o1046–o1048.
12. Desiraju, G. R. *Acc. Chem. Res.* **2002**, *35*, 565–573.
13. Jeffrey, G. A. *An Introduction to Hydrogen Bonding*; Oxford University Press: New York, 1997.
14. SMART *(Version 5.618),* SAINT-*Plus*-NT *(Version 6.04) and* SHELXTL-NT *(Version 6.10)*; Bruker AXS, Madison, Wisconsin, USA.
15. Sheldrick, G. M. *Acta Crystallogr., Sect. A* **1990**, *46*, 467–473.
16. Sheldrick, G. M. SHELXL97; University of Göttingen: Germany, 1997.
17. Bruno, I. J.; Cole, J. C.; Edgington, P. R.; Kessler, M. K.; Macrae, C. F.; McCabe, P.; Pearson, J.; Taylor, R. *Acta Crystallogr., Sect. B* **2002**, *B58*, 389–397.
18. Harris, R. K.; Becker, E. D.; Cabral, S. M. DeM.; Goodfellow, R.; Granger, P. *Pure Appl. Chem.* **2001**, *73*, 1795–1818.